GLIOMA

# Blood-brain barrier opening with neuronavigation-guided focused ultrasound in pediatric patients with diffuse midline glioma



**Cheng-Chia Wu[1,2]*†, Luca Szalontay[3]‡, Antonios N. Pouliopoulos[4]§, Sua Bae[4]¶, Xander Berg[1], Hong-Jian Wei[1]#, Andrea Webster Carrion[3,5], Danae Kokossis[1,6], Chankrit Sethi[3], Jessica Fino[3], Halina Shatravka[3], Jennifer Lipina[3]#, Robin Ji[4], Keyu Liu[4], Omid Yousefian[4], Matthew Gallitto[1], Nina Yoh[7], Zachary Englander[7], Nicholas McQuillan[1], Masih Tazhibi[1], Genesis De Los Santos[1], Peter Canoll[8], Zhezhen Jin[9], James Garvin[3], Robyn D. Gartrell[3,10], Jovana Pavisic[3]**, Alexis Maddocks[11], Angela Lignelli[11], Neil Feldstein[7], Elisa E. Konofagou[4,11,12]*, Stergios Zacharoulis[3]***

**Focused ultrasound (FUS)–mediated blood-brain barrier (BBB) opening with microbubbles is an emerging technology that enables drug delivery for central nervous system diseases. To date, most clinical trials assessing BBB opening in adults were designed to deliver US with a frequency of one treatment over several weeks. Little is known about the feasibility of shorter intervals of US delivery or whether this can be achieved in a pediatric population using a mobile device. Here, FUS and panobinostat were shown to have additive therapeutic effects in a syngeneic orthotopic model of diffuse midline glioma (DMG). We then conducted a single-arm first-in-pediatric trial to investigate the safety and feasibility of delivering neuronavigation-guided FUS treatment in combination with oral panobinostat in children with relapsed DMGs. We included an intrapatient escalation of FUS delivery to assess the feasibility of opening multiple sites in the brain. We demonstrated successful BBB opening using neuronavigation-guided FUS as frequently as every 2 days. Magnetic resonance imaging with contrast was used to identify the region of BBB opening. Three patients were accrued; 22 FUS procedures were delivered for 1 NOTS (number of tumor sites) treated, and four FUS procedures were delivered for 2 NOTS. All three patients received 1 NOTS, without serious adverse events, and two of the patients received 2 NOTS, all without sedation. For 2 NOTS, prolonged BBB opening and one grade 5 event, unlikely related to FUS, were observed. This study demonstrates feasibility of FUS for BBB opening and drug delivery without sedation in pediatric patients.**

## INTRODUCTION

Diffuse intrinsic pontine glioma (DIPG)—a class of tumors more recently reclassified under diffuse midline glioma (DMG) with histone H3 lysine-27–to–methionine (H3K27M) mutation—represents a universally fatal pediatric brain tumor. These tumors arise in midline structures of the brain, most commonly the brainstem, followed by the thalamus and spinal cord. Despite identification of the disease-defining genetic alteration in H3K27M, this knowledge has not resulted in improved treatments (*1*). Apart from the use of radiotherapy (RT) for temporary disease control, no effective systemic treatment exists, and prognosis is dismal with a median overall survival (OS) of 1 year (*1*–*3*). Surgical intervention is limited given the functional importance of the brainstem and the substantial morbidity and mortality associated with its damage. Unlike other high-grade gliomas, DMGs in the brainstem are largely diffuse with microscopic extension into regions of the brain where the blood-brain barrier (BBB) remains relatively intact. This is evidenced by the lack of enhancement on postcontrast T1-weighted magnetic resonance imaging (MRI) with tumors typically visualized on T2-weighted and fluid-attenuated inversion recovery (FLAIR) sequences. This protected location presents many

[1]Department of Radiation Oncology, Columbia University Irving Medical Center, New York, NY 10032, USA. [2]Herbert Irving Comprehensive Cancer Center, New York, NY 10032, USA. [3]Department of Pediatrics, Division of Pediatric Hematology/Oncology/Stem Cell Transplantation, Columbia University Irving Medical Center, New York, NY 10032, USA. [4]Department of Biomedical Engineering, Columbia University, New York, NY 10027, USA. [5]Children's Hospital of Philadelphia, Philadelphia, PA 19104, USA. [6]Department of Pediatrics, Washington University, St. Louis, MO 63110, USA. [7]Department of Neurosurgery, Columbia University Irving Medical Center, New York, NY 10032, USA. [8]Department of Pathology and Cell Biology, Columbia University Irving Medical Center, New York, NY 10032, USA. [9]Department of Biostatistics in Mailman School of Public Health, Columbia University Irving Medical Center, New York, NY 10032, USA. [10]Department of Oncology, Division of Pediatric Oncology, Johns Hopkins University School of Medicine, Baltimore, MD 21287, USA. [11]Department of Radiology, Columbia University Irving Medical Center, New York, NY 10032, USA. [12]Department of Neurological Surgery, Columbia University Irving Medical Center, New York, NY 10032, USA.
*Corresponding author. Email: cw2666@vt.edu (C.-C.W.); ek2191@columbia.edu (E.E.K.); sz2764@cumc.columbia.edu (S.Z.)
†Present addresses: Fralin Biomedical Research Institute, Virginia Polytechnic Institute and State University, Roanoke, VA, USA; Department of Internal Medicine, Virginia Tech Carilion School of Medicine, Roanoke, VA, USA; Department of Biomedical Engineering and Mechanics, Virginia Polytechnic Institute and State University, Blacksburg, VA, USA; Brain Tumor Institute, Children's National Hospital, Washington, DC, USA; Center for Cancer and Immunology Research, Children's National Hospital, Washington, DC, USA; Inova Schar Cancer Institute, Department of Radiation Oncology, Fairfax, VA.
‡Present addresses: Brain Tumor Institute, Children's National Hospital, Washington, DC, USA; George Washington University, School of Medicine and Health Sciences, Washington, DC, USA.
§Present address: School of Biomedical Engineering & Imaging Sciences, King's College London, London, UK.
¶Present address: Department of Electronic Engineering, Sogang University, Seoul, Korea.
#Present address: Fralin Biomedical Research Institute, Virginia Polytechnic Institute and State University, Roanoke, VA, USA.
**Present address: Memorial Sloan Kettering Cancer Center, New York, NY, USA.

treatment challenges for DMGs, including limited bioavailability of systemic therapies (*2*).

The BBB is the brain's natural protective barrier that prevents toxins and infectious agents from reaching the brain parenchyma (*4*–*6*). It acts as a permeability membrane limiting penetrance of molecules larger than 400 Da to the brain parenchyma and therefore creates a barrier for central nervous system (CNS)–based treatments (*7*). In the setting of DMG, the BBB remains relatively intact with some degree of heterogeneity (such as between the pons and thalamus). Potential hypotheses that explain the BBB impermeability for DMG are supported by the low density of capillaries along with membrane expression of functional ATP-binding cassette (ABC) transporter proteins (*8*, *9*). This hinders effective chemotherapeutic and biological agents from reaching the tumor and may contribute to why there are no effective systemic treatments for DMG to date. Focused ultrasound (FUS) offers a safe and noninvasive method of localized BBB opening (BBBO) for drug delivery. Combined with the use of microbubbles (an ultrasound contrast agent), FUS delivery of nonionizing acoustic radiation in the form of low-frequency, nonablative sound waves can achieve local and reversible BBBO to enhance drug delivery in a noninvasive manner by ~4- to 10-fold (*10*). In the presence of ultrasound contrast or microbubbles, the delivery of FUS can cause the microbubbles to rhythmically contract and expand, or enter "cavitation." This process through a variety of postulated mechanisms can lead to temporary and reversible BBBO (*10*). BBBO with FUS has been shown to be feasible in the hippocampus, putamen, and substantia nigra (*11*). We and others demonstrated in preclinical models that FUS-mediated BBBO can also be achieved in the setting of the brainstem (*12*, *13*).

The number of early-phase clinical trials demonstrating safety and feasibility of BBBO in adults has grown since the first US Food and Drug Administration (FDA) approval of a high-frequency ultrasound device for patients with essential tremor in 2018 (*14*). To date, there are four clinically investigated ultrasound devices being tested in the brain for drug delivery including Exablate Neuro from Insightec, SonoCloud and Sonocloud-9 from Carthera, NaviFUS, and UltraNav from Delsona (*12*, *14*). BBBO has been achieved in adult patients with a wide variety of neurological disorders including Alzheimer's disease, amyotrophic lateral sclerosis, and primary and secondary brain tumors (*10*). To date, however, there has been limited experience using FUS in children and specifically in DMGs.

Here, we report a clinical trial using FUS to open the BBB in three pediatric patients with DMGs (*12*). In this study, we treated pediatric patients with progressive DMGs with FUS using the UltraNav FUS device (Delsona) with concurrent oral panobinostat administration. We describe our experience and workflow using the neuronavigation-guided FUS (NgFUS) device in children in an outpatient setting without the use of anesthesia and sedation.

## RESULTS

### FUS and panobinostat show therapeutic effects in a syngeneic orthotopic model of DMG

Using a syngeneic orthotopic model of DMG using 4423 DMG cells from O. Becher (*15*), animals were treated with either vehicle control or panobinostat with or without FUS (fig. S1A). The combination of FUS and panobinostat improved tumor local control as seen on MRI (fig. S1, B and C) and improved OS (fig. S1D). Liquid chromatography–tandem mass spectrometry (LC-MS/MS) was performed in the brainstem tumors and sera of animals treated with panobinostat with or without FUS. A trend for an increase in panobinostat delivery was observed (fig. S1, E and F).

### Clinical trial participants

This single-arm, first-in-pediatric trial (NCT04804709) enrolled five patients, with three ultimately accrued. Demographics of the enrolled patients are summarized in table S1. General clinical characteristics and prior treatments are described in table S2. Two of three patients with DMGs had initial presentation in the brainstem, whereas one patient had thalamic DMG that extended into the brainstem and cerebellum. All patients had received up-front RT and systemic anticancer therapies before study enrollment. One patient received reirradiation before enrollment.

#### *Treatment workflow*

Given that the UltraNav FUS device (Delsona), a new device developed at Columbia University and previously shown to be successful in patients with Alzheimer's disease (*16*), has not been used in the pediatric patient population, a standard operating procedure for patient workflow (Fig. 1A) was developed including patient intake, patient simulation, treatment planning, and FUS delivery. This was largely adapted from the workflow for radiation treatment (Fig. 1B). All patients met with a radiation oncologist and a neuro-oncologist for a joint consultation and were consented for the study. Baseline enrollment labs and tests were performed, and a restaging treatment planning MRI was obtained. Using the Brainsight Software, one or two treatment targets were selected and confirmed at our multidisciplinary pediatric neuro-oncology tumor board. Given that the clinical treatment target volume (CTV) for radiation planning for DMG often extends 1 cm beyond the radiographic findings, the FUS target was selected to be in a region of the brain that was noncontrast enhancing and within 1 cm of the radiographic extent of disease. For all three patients, we targeted the brachium pontis region of disease. Treatment planning took ~1 week, and during this time, the patient was brought in for a patient simulation session in which a dry run was performed for each target to ensure that treatment setup could be achieved. This took place in a standard examining room in the Department of Radiation Oncology. Setup parameters and photos were documented in the simulation worksheet (a mock patient setup is shown in fig. S2, A to E). During treatment planning, patient-specific acoustic simulation was conducted to estimate skull-induced ultrasound attenuation. On the day of treatment, a clinical time-out was performed (in which the patient's name, date of birth, medical record number, the FUS procedure to be performed, and the laterality was confirmed in the treatment room) and the patient was set up as per the simulation worksheet for an initial plan check session to ensure setup parameters before treatment. The FUS site was identified, and an ~5 cm–by–5 cm region was shaved to skin. Degassed ultrasound gel was applied to the transducer, and the FUS device was targeted (fig. S2E). A 10-ml saline flush was delivered using a 10-ml saline syringe, followed by Definity microbubbles and then another 10-ml saline flush. The FUS sonication was initiated 3 s before the microbubble injection and delivered over 2 min (see table S3 for sonication parameters). Microbubble cavitation activity was monitored during this time by the passive cavitation detector (PCD). Microbubble "cavitation" denotes the resulting microbubble oscillation induced by the ultrasound beam that, upon interaction with the microbubble, results in the latter's gas expansion through the incurred pressure change. A neurological exam was performed before and

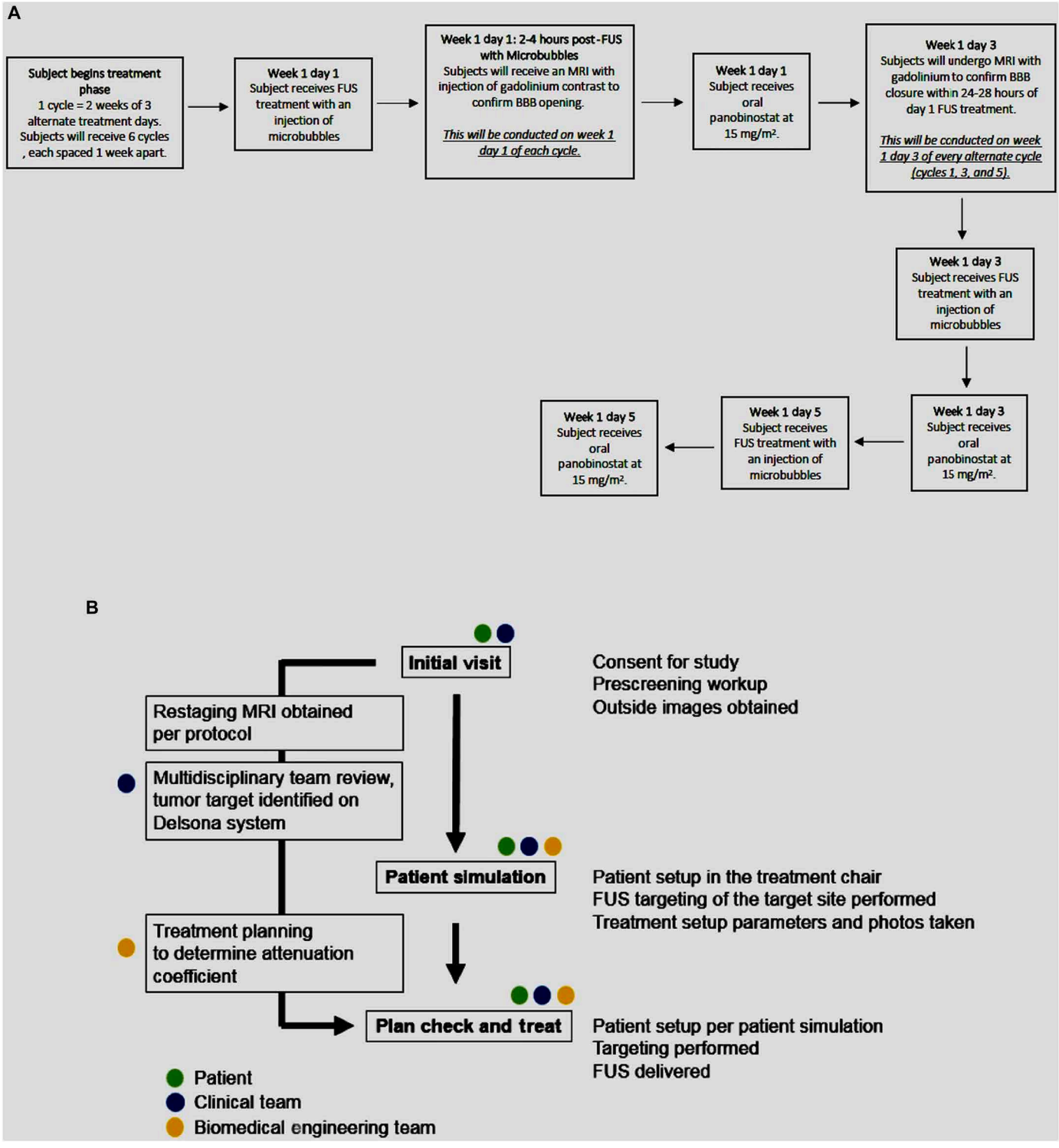


**Fig. 1. Trial design and initial patient workflow.** (**A**) Representative workflow of a single treatment cycle. In total, one to four treatment cycles were completed per patient. For week 2 of each cycle, a similar schema was followed with the exception of MRIs with contrast conducted to evaluate opening and closing of the BBB. Cycles 2 and 4 followed a similar schema with the exception of an MRI to confirm closure of the BBB on day 3. MRI for BBB closure was planned for the first successful BBBO FUS treatment at the beginning of each NOTS level. This was planned per protocol for cycles one, three, and five. (**B**) Sample patient workflow from consultation to treatment. Patient simulation, plan check, and treatment were performed in a standard examining room in the Department of Radiation Oncology.

after ultrasound. Treatments were performed in a standard examining room in the Department of Radiation Oncology where patients remained awake with no anesthesia required.

***Primary outcome***

A tabular presentation of the patients' details is included in data file S1. A total of 26 FUS procedures were performed. MRI was performed with FUS as per protocol. In brief, MRI was performed with the first FUS treatment of cycle 1 and after each number of tumor sites (NOTS) escalation to confirm BBBO. Some FUS delivery attempts did not achieve BBBO, and repeat MRI was performed with the subsequent FUS attempts. In total, post-FUS MRI was performed 16 times. A total of 22 FUS procedures were for 1 NOTS treated, and four FUS procedures were for 2 NOTS (Fig. 2, A and B). Of the three patients accrued, BBBO was achieved in all three patients. In all FUS treatment sessions where BBBO was confirmed by MRI, the volume of the opening was quantified using the T1-weighted postcontrast MRI image (Table 1). The average opening size for 1 NOTS was 0.257 $cm^3$ with a minimum of 0.214 $cm^3$ and a maximum of 0.300 $cm^3$. Two patients proceeded with 2 NOTS FUS procedures. The 2 NOTS sonications of patient 1 were performed ipsilaterally, and although they were separated by a distance greater than the focal spot width (Fig. 2B), the BBBO of the two sites (the trajectory of the two deliveries are depicted by the red arrow) merged, and the quantification of the two openings was recorded cumulatively. Patient 3 was treated contralaterally. The average cumulative opening size of the 2 NOTS targets, when both targets were confirmed open, was 1.433 $cm^3$ with a minimum of 0.799 $cm^3$ and a maximum of 2.440 $cm^3$. In one case of a 2 NOTS procedure, the BBB was confirmed to be open only in the first site, and the opening volume was found to be 0.909 $cm^3$ (Table 1). We did not perform dynamic contrast-enhanced MRI (DCE-MRI) in this study to calculate capillary permeability (K-trans); however, we quantified the percent contrast enhancement (fig. S3). The average percent contrast enhancement increase for 1 NOTS opening was 20.8%, whereas for 2 NOTS, it was 57.1% (Table 1). During each FUS treatment, real-time cavitation monitoring was performed. The PCD monitored the microbubble activity during 2 min of therapeutic ultrasound delivery. The cavitation monitoring showed that all cavitation modes increased between 10 and 35 s, evidencing the microbubble-ultrasound interaction (Fig. 3). The cavitation modes detected were for harmonic, ultraharmonic, and inertial cavitation. For all three patients treated with 1 NOTS, a baseline cavitation characteristic was recorded before the delivery of the microbubble and a rise in cavitation was observed (Fig. 3, A, D, and E). For the two patients who received 2 NOTS treatment, only a single microbubble push was used for both targets. (Fig. 3, B and F) Thus, for the first treatment site of the 2 NOTS, a rise in cavitation was observed as in patients who only received 1 NOTS treatment. Doses of all cavitation modes increased between 10 and 35 s, indicating microbubble and ultrasound interaction after microbubble perfusion into the focal volume. For the second treatment site (Fig. 3, C and G), cavitation doses were stable or steadily declining throughout the duration of the sonication. No increase from baseline was expected because microbubbles were already present in the bloodstream. During all treatments, we did not observe that signals of inertial cavitation dose (ICD) increased above those of stable cavitation [using stable harmonic cavitation dose (SCDh) or stable ultraharmonic cavitation dose (SCDu)].

A complete list of treatment emergent adverse events (AEs) attributed to FUS or panobinostat is reported in Table 2. In relation to FUS, BBBO using a NgFUS system and Definity microbubbles was, overall, well tolerated by the patients. One AE was attributed to FUS: a Common Terminology Criteria for Adverse Events (CTCAE) 5.0 grade 1 event of transient skin erythema and dysesthesia at the point



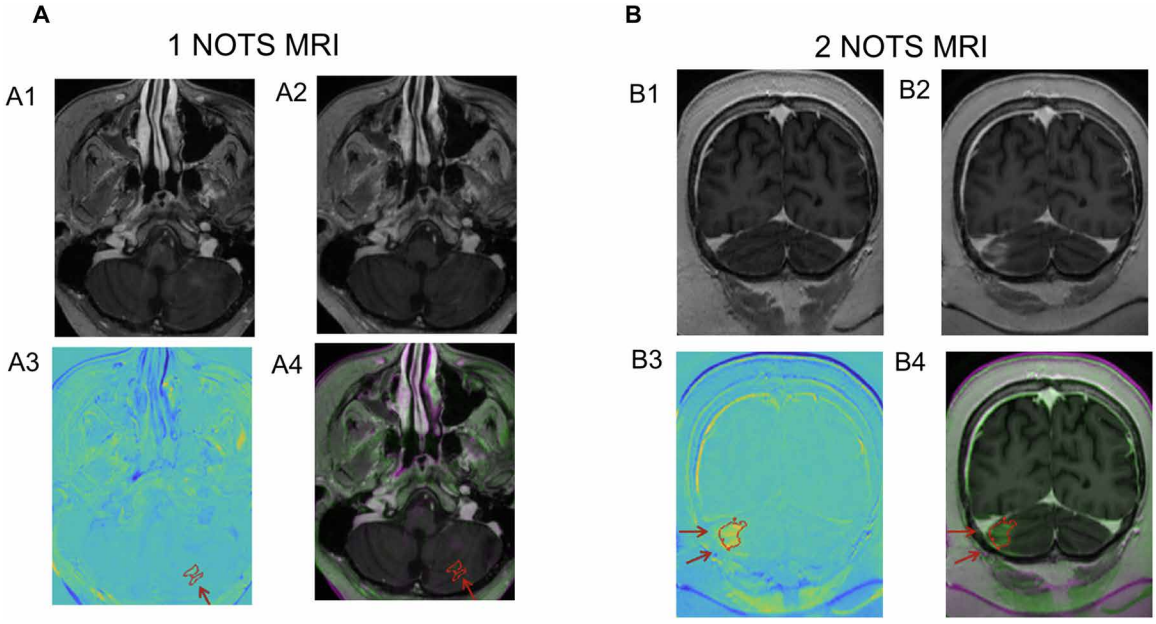


**Fig. 2. MRI demonstration of BBB opening.** (**A** and **B**) Representative MRI images to illustrate BBBO for 1 NOTS from patient 2 (volume: 0.214 $cm^3$, contrast 126%; MRI axial slice) (A) and 2 NOTS from patient 1 (merged volume 2.44 $cm^3$, contrast 180%, MRI coronal slice). BBB opening was defined as areas of new T1-weighted postcontrast enhancement along the trajectory of the FUS delivery. (i) Baseline postgadolinium T1-weighted image. (ii) Posttreatment postgadolinium BBBO T1-weighted image. (iii) Subtracted image of 1 and 2 with the quantified BBBO contoured in red. (iv) Overlaid image of 1 and 2 with the quantified BBBO contoured in red. The red arrow represents the focused ultrasound beam path for each FUS treatment.

**Table 1. Key parameters of BBB opening sessions.** BBBO was confirmed by MRI, and the volume of the opening was quantified using the T1-weighted postcontrast MRI image. –, not applicable.

| NOTS | BBB determination | Total procedures | Volume opening ($cm^3$) average (min-max) | %Contrast enhancement (*5*) (min-max) | Treatment to opening confirmation time (hours) average (min-max) | Treatment to closing confirmation (hours) average (min-max) | Treatment duration (min) average (SD) |
|---|---|---|---|---|---|---|---|
| 1 NOTS | Confirmed open | 3 | 0.257 (0.214–0.300) | 20.8 (12.6–30.7) | 4.46 (3.9–5.5) | 37.2 (33.5–42) | 47.7 min ± 12.8 |
| | Confirmed not open | 6 | – | – | 2.5 (1.5–3.7) | – | |
| | Not paired with MRI | 13 | – | – | – | – | |
| 2 NOTS | Confirmed open (2/2) | 3 | 1.433 (0.799–2.44) | 57.1 (334.1–80.2) | 1.7 (1.6–2.4) | 118.8 (86–174) | 83.5 min ± 18.7 |
| | Confirmed open (1/2) | 1 | 0.909 | – | 2.4 | 98.5 | |
| | Confirmed not open | 0 | – | – | – | – | |
| | Not paired with MRI | 0 | – | – | – | – | |

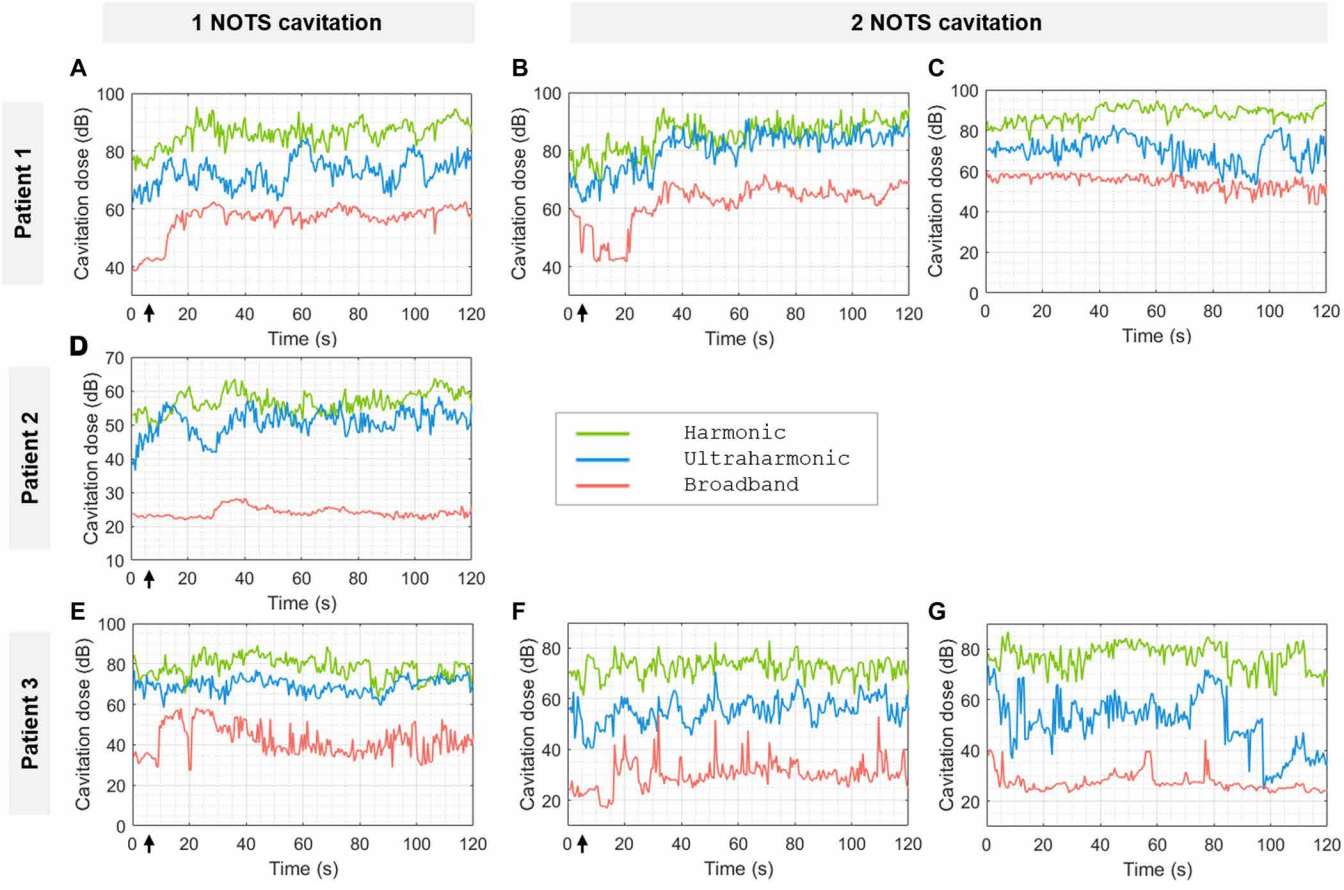


**Fig. 3. Real-time cavitation monitoring during FUS.** (**A** to **G**) Representative cavitation recordings for all three patients for 1 NOTS FUS treatment [(A), (D), and (E)] or 2 NOTS FUS treatment [(B) and (F) are the recordings for the first site, and (C) and (G) are the recordings for the second site]. The traces show the recorded cavitation dose over 2 min. The green trace represents harmonic, the blue trace represents ultraharmonic, and the red trace represents broadband cavitation. Microbubble injection occurred at ~3 s (arrow) and resulted in an increase in all three modes of cavitation at ~10 s when the microbubbles reached the brain target.

**Table 2. List of adverse events (*n* = 3).** LDH, lactate dehydrogenase.

| Toxicity | Grade of event | Number of patients affected | Attributed to drug | Attributed to device |
|---|---|---|---|---|
| Anemia | 3 | 1 | Probably related | Unrelated |
| Alanine aminotransferase increased | 2 | 1 | Possibly related | Unrelated |
| Aspartate aminotransferase increased | 3 | 1 | Possibly related | Unrelated |
| Blood bicarbonate decreased | 1 | 1 | Unlikely related | Unrelated |
| Blood LDH increased | 1 | 1 | Unlikely related | Unrelated |
| Bradycardia | 1 | 1 | Unlikely related | Unrelated |
| Cardiac arrest | 5 | 1 | Unlikely related | Unrelated |
| Diarrhea | 1 | 1 | Probably related | Unrelated |
| Dry eye | 2 | 1 | Unlikely related | Unrelated |
| Dry mouth | 1 | 1 | Unlikely related | Unrelated |
| Dyspepsia | 2 | 1 | Possibly related | Unrelated |
| Flushing | 2 | 1 | Possibly related | Unrelated |
| Headache | 1 | 1 | Unlikely related | Unrelated |
| Hyperglycemia | 1 | 3 | Unlikely related | Unrelated |
| Hypermagnesemia | 1 | 2 | Probably related | Unrelated |
| Hyperphosphatemia | 1 | 1 | Probably related | Unrelated |
| Hypoalbuminemia | 1 | 3 | Probably related | Unrelated |
| Hypocalcemia | 2 | 1 | Probably related | Unrelated |
| Hypokalemia | 3 | 1 | Probably related | Unrelated |
| Hypomagnesemia | 1 | 1 | Possibly related | Unrelated |
| Hyponatremia | 1 | 2 | Probably related | Unrelated |
| Hypophosphatemia | 1 | 1 | Probably related | Unrelated |
| Hypoxia | 3 | 1 | Unlikely related | Unrelated |
| Infections and infestations, other COVID-19 | 3 | 1 | Unlikely related | Unrelated |
| Lymphocyte count decreased | 3 | 2 | Probably related | Unrelated |
| Nausea | 1 | 3 | Probably related | Unrelated |
| Otitis media | 2 | 3 | Unlikely related | Unrelated |
| Platelet count decreased | 1 | 1 | Probably related | Unrelated |
| Skin and subcutaneous tissue disorders, other excoriation | 1 | 1 | Unlikely related | Unrelated |
| Skin and subcutaneous tissue disorders, other irritation | 1 | 1 | Unrelated | Definitely related |
| Urinary tract infection—*Escherichia coli* | 3 | 1 | Unlikely related | Unrelated |
| Vomiting | 2 | 1 | Probably related | Unrelated |

of contact with the transducer was documented in one patient after treatment and resolved without intervention. There were no further toxicities or AEs related to FUS. Overall, the treatment-related events observed were similar to the known toxicity profile of panobinostat. However, one grade 5 event occurred. The event was reviewed by Columbia University Medical Center's Data and Safety Monitoring Committee (DSMC) and was characterized as a likely thromboembolic event. Autopsy was offered to the parents, which they deferred. Risk factors for thromboembolic events included severe COVID infection requiring prolonged hospitalization, obesity due to steroid use, and limited mobility. In addition, panobinostat could have contributed to the event given its association with cardiac arrhythmias, myocardial infarction, and cardiac arrest. FUS was delivered 6 days before this patient's death, with no sign of acute neurological or systemic side effects. Serial MRI had shown near-complete closure of the site treated with resolution of the T1-weighted postcontrast enhancement and residual T2-FLAIR hyperintensity 2 days before the patient's death (fig. S4). DSMC review determined that it was unlikely related to FUS.

### *Secondary outcome*

Using the UltraNav FUS device (Delsona, USA), all FUS treatments were delivered as an outpatient procedure in the Department of

Radiation Oncology. The mean treatment package time (from the patient entering the treatment room to exiting the room, including patient setup, registration, pretreatment targeting validation, and completion of the FUS delivery) when targeting one site was 47.7 ± 12.8 min. When targeting two sites, the mean treatment package time was 83.5 ± 18.7 min. The ultrasound delivery time for each FUS treatment was 2 min per target. Using Brainsight, we analyzed the degree of movement during the ultrasound delivery to assess the targeting precision (Fig. 4). Over the course of the study, the average maximal distance was 4.10 ± 3.82 mm, whereas the average mean absolute deviation (MAD) during each treatment was 1.01 ± 0.90 mm. Previous FUS studies have largely limited FUS treatment to one treatment per month. We performed FUS treatment as frequently as every other day, for up to 2 weeks at a time. One phenomenon we noted in our study was that the BBB closure when targeting 2 NOTS was delayed longer than with 1 NOTS treatment. For all three patients who received 1 NOTS FUS treatment and achieved BBBO, BBB closure was confirmed at the first closure MRI image 2 days after FUS delivery. However, for 2 NOTS treatment, prolonged BBBO was observed. For all 2 NOTS treatments that achieved BBBO, BBB closure was delayed beyond 2 days after FUS delivery. For two of the 2 NOTS treatment, BBB closure was confirmed at 4 days after FUS delivery. For one of the 2 NOTS treatment, BBB closure was near complete at closure MRI 4 days after FUS delivery (Fig. 5 and fig. S4). During the study, two patients had radiographic tumor control. One patient had early progression during cycle one. The two patients who had temporary local control had disease limited to the brainstem. Similarly, both patients had symptomatic improvement (Table 3). The study was closed prematurely because the approval of the new drug application (NDA) for panobinostat was withdrawn by request from Secura Bio Inc. in the United States (*17*).

## DISCUSSION

DIPG/DMG is a fatal brain tumor mainly found in children without any progress in treatment despite decades of research. Various reasons account for this failure including, but not limited to, the infiltrative and heterogeneous nature of the tumor, the anatomical location of the disease, and the complex biology in part characterized by epigenetic modifications that predispose cells to pro-oncogenic changes in gene expression. There is failure to achieve effective intratumoral concentrations of cancer fighting drugs because of the BBB. This feasibility study attempts to address this BBB limitation through the use of FUS while using one of the most effective epigenetic modifiers in vitro.

With the development of a clinical device to target the brain, there has been a rise in interest in the applications of low-intensity FUS (LIFU) and, since then, has led to multiple clinical trials exploring the use of different clinical devices to deliver low-frequency ultrasound for the purpose of opening the BBB. There are three general classes of clinical devices that are in clinical trials for BBBO and



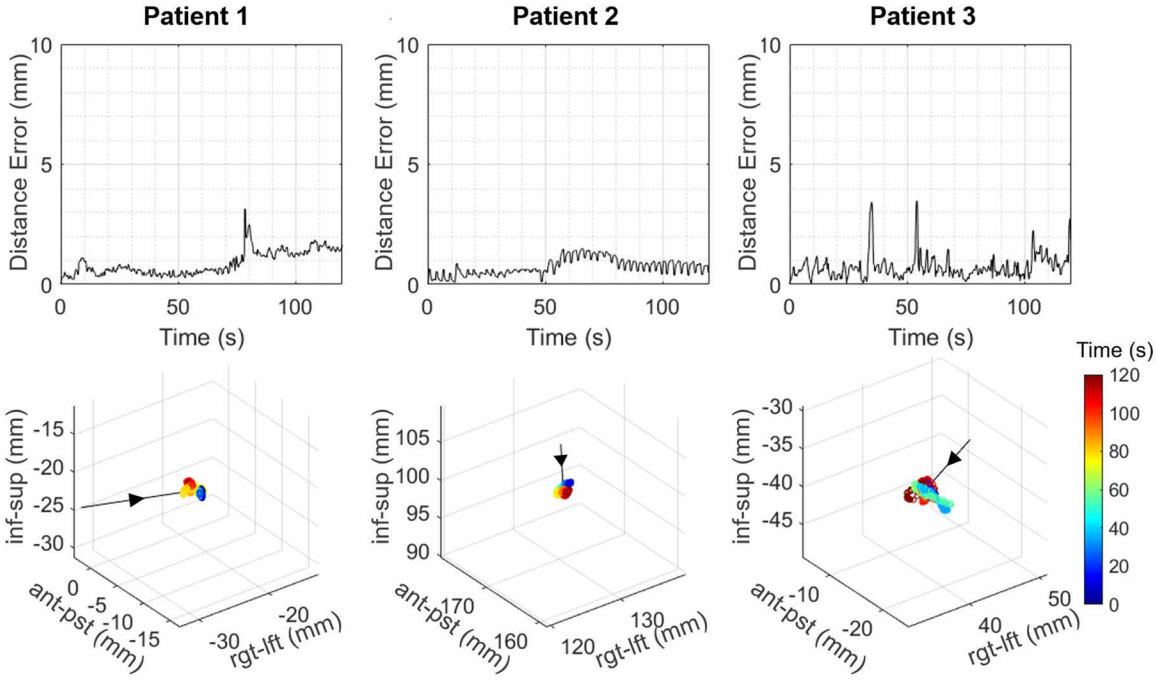


**Fig. 4. Analysis of real-time monitoring of movement during FUS.** During FUS delivery, movement of the transducer target was monitored in real time using Brainsight. The top row shows the movement of the FUS focus (distance error in mm) from the initial focal position recorded during the 2 min of treatment for all three patients. The bottom row displays the 3D position of the focus relative to the patient's head tracked for 2 min. Representative tracing and 3D analysis for all three patients are shown. The time is indicated by the color of the dots. The arrow indicates a vector of movement. This is not normalized. Inf-sup, inferior-to-superior axis; ant-pst, anterior-to-posterior axis; rgt-lft, right-to-left axis.

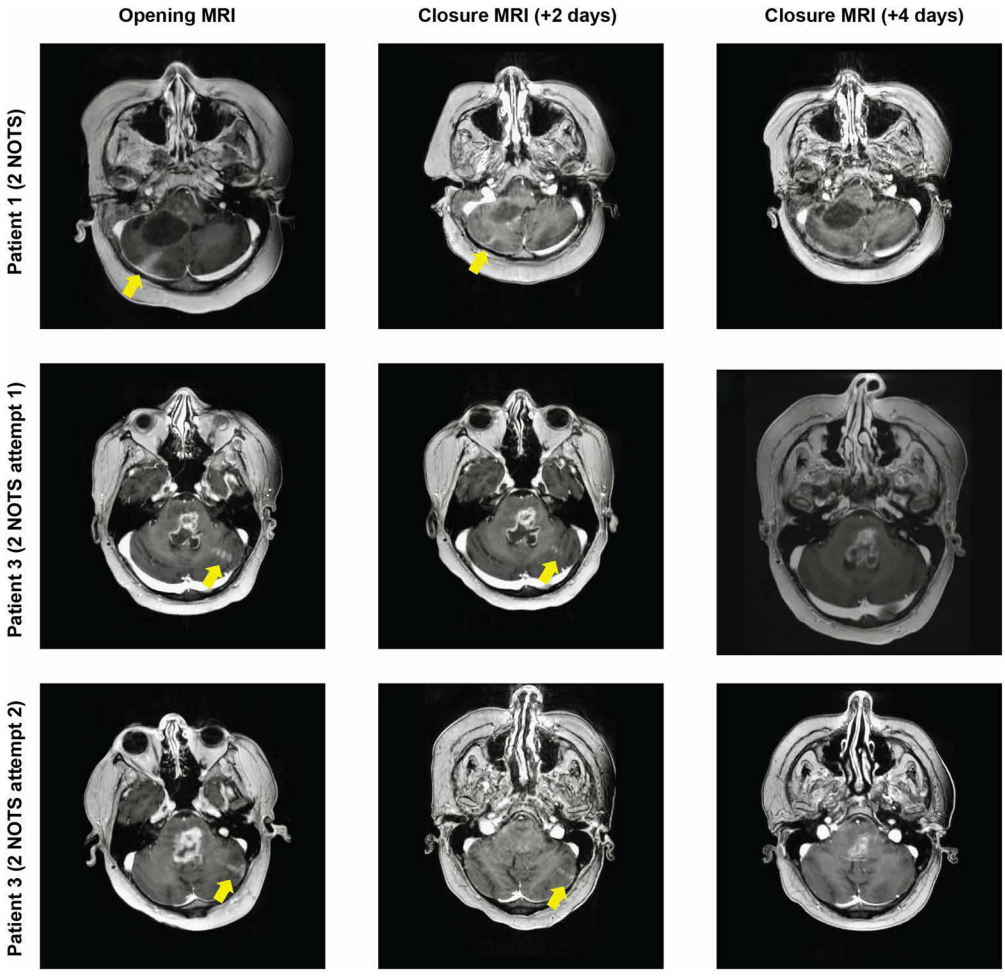


**Fig. 5. Prolonged latencies to achieve BBB closure were observed when treating 2 NOTS.** Shown are representative MRI images from patients 1 and 3 treated with FUS for 2 NOTS; patient 3 underwent two attempts of 2 NOTS BBBO. MRI images were obtained after FUS treatment to verify BBB opening as well as 2 and 4 days posttreatment to verify subsequent closure. BBB opening was defined as areas of new T1-weighted postcontrast enhancement along the trajectory of the FUS delivery (yellow arrow). BBB closure was defined as resolution of the contrast enhancement as defined by BBB opening.

drug delivery. These include MRI-guided FUS (MRgFUS), implantable non-FUS devices, and NgFUS devices. These devices have been extensively used to achieve BBBO in adult patients with brain tumors (primary or secondary) and other neurological diseases in early-phase clinical trials (*10*). In preclinical studies, the use of LIFU for BBBO has been shown to achieve a 5- to 10-fold increase in drug delivery. Sonabend *et al.* further validated this intraoperatively in humans, in which a 3.7-fold increase in albumin-bound paclitaxel and a 5.9-fold increase in carboplatin were detected in patients with glioblastoma who received the aforementioned systemic therapy when comparing peritumoral tissues treated with or without ultrasound (*18*). More recently, the usage of FUS-guided delivery of antibody targeting amyloid-β (Aβ) for patients with Alzheimer's disease demonstrated focal clearance of Aβ, demonstrating the proof of concept of selected delivery of an antibody for a localized clinical response (*19*).

Clinical and preclinical studies associated with LIFU, to date, have largely been limited to adult patients. Depending on the type of device used, there are differences in their capabilities ranging from frequency of use, treatment time, volume of BBBO, and invasiveness of procedure. Very little is known regarding pediatric patients, in particular patients with relapsed DMGs. Preclinical studies from our group and others demonstrated the safety and feasibility of FUS-mediated BBBO in animals with brainstem gliomas (*11*, *13*, *18*–*21*). More recently, a variety of studies have shown increased drug delivery for DMG including, but not limited to, doxorubicin, etoposide, and panobinostat (*13*, *20*, *22*, *23*). The questions that remain are whether children can tolerate FUS treatment and whether BBBO is feasible. Furthermore, when working with pediatric patients, different considerations include ease of use, anatomical limitations when targeting brain tumors, treatment package time, degree of invasiveness of the therapy, patient tolerance, and need for anesthesia. In addition, the frequency of FUS delivery needs to be guided by the appropriate pharmacokinetic and dynamic data of the agents used for therapy. Many therapeutic agents are given daily, and the question remains whether opening the BBB with FUS in more frequent intervals is feasible.

In this study, we elected to use panobinostat to combine with FUS. Panobinostat is a histone deacetylase inhibitor that has shown promise in treating DMG in vitro through multiple drug screening studies (*24*). Although panobinostat was found to be efficacious in vitro, it had limited therapeutic benefit in patients with DMGs and has limited penetrance into the brain parenchyma (*16*, *25*). We and others have shown that FUS can enhance panobinostat effects in preclinical models of DMG. Whereas we showed that FUS combined with panobinostat led to a local control benefit with a survival benefit in preclinical models for DMG (fig. S1), Martinez *et al.* further demonstrated an increase in delivery of panobinostat with FUS

**Table 3. Treatment course for all three patients.** –, not applicable.

| Patient | Cycles completed | 1 NOTS treatment | 2 NOTS treatments | Clinical benefit | Survival time from first FUS treatment | Survival time from last FUS treatment | Cause of death | Progression-free survival |
|---|---|---|---|---|---|---|---|---|
| 1 | 6 (5 with FUS) | 12 | 2 | Muscle weakness in the upper limb improved from baseline grade 3 to grade 2; head tremor improved from grade 2 to grade 1; dysarthria improved from grade 2 to grade 1 | 192 days | 87 days | COVID-19 related, off study | 142 days |
| 2 | 1 | 6 | 0 | – | 91 days | 80 days | DMG disease progression, off study | 16 days |
| 3 | 4 (3 with FUS) | 4 | 2 | Dysarthria improved from grade 2 to grade 1; muscle weakness in the lower limb (hip flexion) improved from grade 3 to grade 2 | 70 days | 7 days | COVID-19 related, on study | Death before progression |

into the brain parenchyma and achieved prolonged survival benefit in preclinical studies (*22*). The FUS system we used in the mouse model differed from the system used for patients given the distinct size of the brain and skull among the two species (16). Given that UltraNav is functioning with an investigational new drug (IND), we were limited by the safety parameters of using the lowest derated peak-negative pressure for BBBO of 0.2 MPa, whereas a higher pressure was used in the preclinical models (*13*). There are some similarities and differences between our approach and that of Martinez and colleagues. Both groups used a 1.5-MHz transducer with a pressure of 0.6 MPa; however, Martinez and colleagues delivered FUS once a week, whereas we delivered FUS twice a week. In our clinical trial, we had proposed escalating the NOTS to increase the volume treated. Thus, in our preclinical model, we delivered 4 NOTS in a 1-mm lateral–by–2-mm anterior/posterior grid surrounding the targeted tumor to ensure adequate BBBO, in contrast with a single focus used by the Martinez group. The pressures used in both preclinical models were higher than what was used with the clinical device given that the investigational device exemption required a lower acoustic pressure. Whereas Martinez *et al.* elected to use a human DIPG cell line, BT-245, orthotopically engrafted into the brainstems of immunocompromised mice, our priority was to test the safety and feasibility of FUS-mediated panobinostat delivery. We selected a syngeneic orthotopic xenograft model of DMG using the 4423 DMG cells received from O. Becher (*15*). Repeated FUS treatment with panobinostat was well tolerated without increased morbidity or mortality. It is unknown whether an intact immune system altered the therapeutic effects of FUS-mediated delivery of panobinostat, and more studies are needed.

Along with the mechanistic potential of panobinostat, one of our goals for the clinical study presented here was to select a therapy that can be given orally in the outpatient setting to couple with outpatient-based FUS delivery. In this trial, panobinostat was given orally 3 days a week (Monday-Wednesday-Friday) for 3 weeks with a 1-week break per cycle (*16*). Most clinical trials using various ultrasound devices have limited the number of BBBO to approximately one opening per month, and a FUS BBBO strategy to couple with a drug given daily was needed. Because panobinostat is taken 3 days a week, we wanted to increase the frequency of our FUS-mediated BBBO to optimize the duration of increased panobinostat delivery to the target. In our preclinical study, we delivered panobinostat four times a week to prolong systemic circulation of panobinostat with FUS twice a week to prolong BBBO and drug delivery to the tumor target, and treatments were well tolerated. To date, BBBO across various clinical devices has been reported to last as short as 6 hours, with BBB closure occurring at ~24 to 48 hours (*19*, *26*–*28*); hence, we elected to design our study to deliver FUS Monday-Wednesday-Friday to maintain tumor exposure to panobinostat with presumed adequate timing for BBB closure between treatments. MRI images for verifying BBBO and BBB closure were only performed during the beginning of each NOTS escalation. Given the risk for gadolinium toxicity, it was not feasible to perform MRI after each FUS treatment.

In this study, we achieved BBBO in all three patients treated. FUS was delivered every other day and was well tolerated. We delivered a

total of 26 treatments. Patients with limited performance status also tolerated treatment, and all treatments were performed in the outpatient setting in the Department of Radiation Oncology without anesthesia or sedation. With our immobilization strategy, patient movement during treatment was effectively limited, resulting in precise targeting with a minimal deviation (MAD = 1.01 + 0.90 mm). Only one patient had a grade 1 scalp irritation during one of the FUS treatments. At 1 NOTS, BBB closure was confirmed with MRI 48 hours after FUS delivery for all three patients; however, for two of the patients who received 2 NOTS treatment, prolonged BBBO was observed. Before this study, prolonged BBBO from repeated clinical FUS delivery had yet to be described, and the time interval for BBBO was thought to be limited to within 24 to 48 hours. For these reasons, we designed our study to perform BBBO and BBB closure MRI at each escalation of NOTS. To date, the use of MRI with contrast is the standard mechanism for verifying FUS-mediated BBBO and BBB closure. Because gadolinium-based contrast is potentially nephrotoxic, it is not clinically feasible to perform scans after every FUS treatment; therefore, our treatments and strategies required balancing the frequency of FUS delivery and MRI. One approach to allowing more frequent MRIs for BBBO confirmation is using deep learning to model contrast enhancement from BBBO in a reduced contrast agent dose setting (*29*). Further studies are needed before clinical application.

The exact mechanism for why prolonged times to achieve BBB closure were observed with 2 NOTS treatment is unknown; however, one possibility could be the frequent FUS deliveries. The observation of prolonged BBBO was seen in later treatment cycles when patients had received multiple successful FUS deliveries. FUS-mediated BBBO, in part, is due to the cavitation effects of the microbubbles leading to mechanical interactions resulting in BBBO; however, FUS has also been shown to affect the expression of adhesion molecules and to modulate the immune system, all of which contribute to the restoration of the BBB (*30*, *31*). Another possibility is that, with 2 NOTS treatment, there may be off-target effects of sound waves that reflect off the calvarium, contributing to further BBBO. Now, in our second clinical trial using etoposide and FUS (*32*), we are determining the BBB closure time at the beginning of each cycle to tailor the frequency of ultrasound delivery. These findings are important for consideration for clinical trial designs for ultrasound-mediated BBBO that are planning to either deliver more frequent ultrasound treatments or deliver multiple treatments in one setting.

Although the volume of BBBO achieved with UltraNav is small, very little is known regarding the volumetric size of BBBO and its correlation to clinical outcomes. Of the three patients we treated, the two patients with clinical improvement had disease localized to the brainstem, whereas the patient with disease progression had thalamic involvement. Whether larger areas of BBBO are necessary depending on the extent of anatomical involvement needs to be explored. Our strategy for opening a larger volume involves treating higher NOTS. Other strategies are now being explored including the usage of acoustic holograms to offer intensity-modulated ultrasound (IMUS). We began exploring the potential of using IMUS for brainstem patients because this may be an option to increase treatment volume (*33*–*36*).

Given that we were targeting brainstem disease through the cerebellum, our treatment approach was through the posterior/lateral head. Depending on the anatomical variation, the coupling of the transducer may not have been completely flat and may have abutted the soft tissue neck. More understanding of how this may affect the calculation of the attenuation coefficient is necessary for NgFUS treatments that may not target the frontal lobe.

Our study has limitations. Panobinostat was removed from the US market, and we had to terminate the study early. In addition, this study occurred during the height of the COVID-19 pandemic as the medical field was determining strategies to manage the infection. One patient had contracted COVID-19 while on study and required prolonged hospitalization, whereas a second patient had contracted COVID-19 once off study. Although many of the precautionary steps regarding COVID-19 and this trial were adjusted on the basis of the understanding of the disease, there has since been more information on the acute and late risks associated with COVID-19. Risks associated with COVID-19 infection should be considered in future studies.

Despite this, our study has since led to a growing interest in using FUS for the treatment of DIPG/DMG and other pediatric brain tumors. Other studies using different devices are ongoing (ClinicalTrials.gov identifier: NCT05293197, NCT05630209, and NCT05615623) (*12*). We have since opened our second phase 1 trial using UltraNav specifically testing the use of etoposide for patients with relapsed DIPGs/DMGs (ClinicalTrials.gov identifier: NCT05762419). With the rising interest in the use of ultrasound for BBBO for patients with DIPGs/DMGs, the Focused Ultrasound Foundation led a Focused Ultrasound for DIPG Workshop in October 2021, which was recently reported (*12*). Four devices were discussed: UltraNav (Delsona), Exablate Neuro (Insightec), SonoCloud (Carthera), and NaviFUS. Both UltraNav and NaviFUS use neuronavigation to target the treatment site and guide the ultrasound delivery in a noninvasive manner. Such targeting can be user dependent for accuracy, precision, and time. The UltraNav system uses a single-element transducer for therapeutic delivery with an additional PCD, whereas the NaviFUS system uses a 256-element array with active cavitation monitoring and control. NaviFUS has not been tested on pediatric patients to date; however, neither system needs full cranial immobilization, and treatments can be delivered in the office as an outpatient procedure without sedation. The treatment times are generally shorter with neuronavigation-based targeting devices, as opposed to MRgFUS; however, to date, smaller volumes of BBBO have been achieved. Theoretically, larger BBBO can be achieved with an increased number of targets delivered; this would increase treatment times. SonoCloud is an implantable ultrasound device that is placed surgically with neuronavigation at the time of surgical resection of the brain tumor. Once implanted, the treatments are delivered without image guidance as an outpatient procedure in which a transdermal needle connected to an external power source is attached to the implanted device for treatment. The treatment is delivered over 4.5 min and is the fastest among the devices given that the device is surgically placed and no imaging or targeting is necessary. Large volumes of BBBO have been achieved by using multiple transducer elements (Sonocloud-9), albeit the region of BBBO is limited by the device, with no ability to change the shape of the target to cover irregular or multiple lesions (*10*). Another limitation of the device is that the placement of the device is surgical and limited by the anatomical placement of the device. This may limit the ability to target select structures in the brain. There are no studies using SonoCloud for DIPG/DMG; however, there is a study testing the safety of repeated BBBO for pediatric patients with supratentorial malignant brain tumors. The Exablate Neuro Type 2 (Insightec) is a MRgFUS system that

uses an MRI-compatible helmet that houses a 1024-element LIFU transducer. The system uses real-time MRI to limit ultrasound delivery to the targeted regions while sparing treatment to nontargeted regions. In addition, cavitation threshold detection and spatial mapping allow for homogeneous ultrasound delivery for BBBO. Large volumes of BBBO have been achieved in adult patients (*12*). There are now two phase 1 clinical trials for patients with DIPGs/DMGs in which doxorubicin is delivered. Although unpublished, reports of successful delivery have been reported (*37*), and one limitation for pediatric patients is that head stabilization is required; thus, for pediatric patients undergoing longer treatments, sedation is required (*12*).

With the potential for improving drug delivery for DIPG/DMG, new strategies prioritizing effective therapies are needed, including considering small molecules, biological agents (such as antibodies), adoptive cellular therapy, targeted gene therapy, and more. This includes leveraging the rapidly growing transcriptional and epigenetic characterization of these tumors, including analyses with single-cell RNA sequencing, along with potential partnerships with computational and systems biologists to help identify promising drug targets (*38*). Furthermore, understanding how to combine FUS with standard-of-care RT is critical to help improve treatment options (*39*). The different clinical devices for BBBO have various advantages and challenges when treating pediatric patients with DIPGs/DMGs, and the optimal device is yet to be determined. Some considerations proposed at the Focused Ultrasound Foundation DIPG meeting included three-dimensional (3D) spatial monitoring and control of bubble activity, treatment planning that considers standing waves and allows exposure optimization, a method of quantification of skull properties, incorporating technology and methodology to better quantify drug delivery, establishing a system to avoid full head immobilization, and treatment strategies to allow therapy outside of the MRI environment. Lessons learned from this work can lead the effort toward translating combinatorial treatment approaches to improve outcomes for children with this fatal disease. In conclusion, NgFUS delivery–mediated BBBO is feasible as an outpatient procedure with patients with progressive DIPGs/DMGs.

## MATERIALS AND METHODS

### Study design

#### *Clinical trial*

This was a prospective, single-center, nonrandomized, single-arm feasibility clinical trial, at the Columbia University Irving Medical Center (CUMC) (NCT04804709). The protocol was developed, and data were collected and analyzed by the investigators. The study was conducted in accordance with the Declaration of Helsinki, International Conference of Harmonisation, Good Clinical Practice guidelines, and applicable regulatory requirements. An independent data and safety monitoring committee conducted monitoring of patient safety data. The CUMC institutional review board oversaw trial conduct and documentation (IRB#AAAS5953). All patients or legal guardians provided written informed consent and assent, when appropriate, before participating in the trial.

The minimum enrollment approved was three patients with a maximum of 10 patients. Eligible patients met specific inclusion criteria, including age 4 to 21 years and evidence of clinical or radiographic progression of DMG after standard radiation therapy. In addition, patients had to have fully recovered from the acute toxic effects of all prior anticancer therapy before enrollment. Time from prior therapy was determined as per standardized clinical guidelines. Further details of eligibility criteria are listed in the protocol (data file S2).

Participants in the study were eligible for up to six cycles of FUS and oral panobinostat combination therapy. Panobinostat was obtained from Secura Bio Pharmaceuticals. We adhered to the recommended dosing schedule for panobinostat at a dose of 15 mg/m$^2$, with a maximum dose of 20 mg, to be administered orally on Monday, Wednesday, and Friday of each treatment week. The treatment regimen was designed on the basis of the timing of FUS application and panobinostat's pharmacokinetics. Patients were treated with FUS on the same alternate weekdays before receiving oral panobinostat. The duration of each cycle was 2 weeks followed by a 1-week break. The study followed a NOTS escalation scheme in reference to the number of sites targeted with FUS to open the BBB. An intrapatient escalation design was chosen in which two cycles of one area of tumor target or NOTS was treated. If the BBBO was successful, the following two cycles of treatment were treated with 2 NOTS, followed by 3 NOTS at the final two cycles as described in the protocol (data file S2). A schematic of the treatment schedule is presented in Fig. 2.

The primary outcome was to evaluate the safety and feasibility of using FUS to open 1, 2, or 3 NOTS with three times a week administration of panobinostat in children with progressive DMG. Evaluation of safety was performed by capturing all treatment-related AEs. AEs were assessed through physical and neurological examinations, laboratory studies, and neuroimaging studies. All AEs were graded as per the Common Terminology Criteria for Adverse Events version 5.0 (CTCAE 5.0). Feasibility of BBBO using NgFUS was evaluated by changes in pattern of contrast enhancement, seen on T1-weighted MRI. The secondary outcomes were progression-free survival (PFS), OS, volumetric analysis of BBBO on MRI, treatment package time as defined as the time from patient entering the room to the patient leaving the room, and Brainsight tracking data.

The patient was brought into the outpatient clinic for enrollment and eligibility screening. Each patient was reviewed at our institutional pediatric neuro-oncology tumor board. The principal investigator obtained informed consent and assent, as appropriate. Patients then underwent eligibility screening. Physical and neurological exams were completed by the pediatric neuro-oncologist, nurse practitioner, or the pediatric radiation oncologist. Data analysis was done descriptively.

#### *Preclinical study*

Animal protocols were approved by the Columbia University Irving Medical Center Institutional Animal Care and Use Committee (AC-AABP4566). To generate the DMG mouse model, male 6- to 8-week-old B6 (Cg)-Tyrc-2J/J albino mice from the Jackson Laboratory were orthotopically injected with 4423 DMG cells as previously described (*39*). To validate tumor growth, a 9.4-T MRI system (Bruker Medical, Boston, MA, USA) was used in which weekly T2-weighted images were obtained using a T2-weighted TurboRARE sequence at day 14 postinjection. The free, open-source platform 3D Slicer (www.slicer.org) was used to quantify tumor volume (*39*). Mice were randomized after tumor establishment for treatments. The animals were divided into four groups: vehicle control, FUS alone, panobinostat alone, and panobinostat plus FUS. Two doses of 0.2 ml of panobinostat (10 mg/kg; Selleck Chemicals LLC, Houston, TX, USA) were administered immediately and the day after the sonication. The vehicle of panobinostat is composed of 5% DMSO (dimethyl sulfoxide; Thermo Fisher Scientific,

Waltham, MA, USA), 40% PEG-300 (polyethylene glycol, molecular weight 800; Selleck Chemicals LLC, Houston, TX, USA), 5% Tween 80 (Selleck Chemicals LLC, Houston, TX, USA), and 50% double-distilled water. Tumor-bearing mice received sonication for BBBO on days 17, 21, and 24 postinjections. FUS was delivered using a single-element, spherical-segment FUS transducer driven by a function generator through a 50-dB power amplifier (37). Panobinostat concentrations in the serum and the brain were detected using LC-MS/MS as previously described (*13*). Briefly, tumor-bearing animals were treated with FUS for BBBO 14 days after tumor implantation. Panobinostat (20 mg/kg) was intraperitoneally administered right after FUS sonication. At time points of 15, 30, and 60 min after treatment, the serum and brainstem were harvested for LC-MS/MS. The animal study was not blinded. Animals did not develop tumors after injections were excluded. For each experiment, mouse numbers and statistical tests are described in the figure legends.

### NgFUS procedure

The BBBO procedure was performed using UltraNav (Delsona), a NgFUS system, as previously described (*40*, *41*). In summary, a single-element FUS transducer (model: H-231, Sonic Concepts) was operated at 0.25 MHz (radius: 55 mm; geometric focal depth: 110 mm; focal length: 49 mm; focal width: 6 mm) and driven by a function generator (33500B Series, Agilent Technologies) through a 55-dB radiofrequency power amplifier (A150, E&I). A polycarbonate coupling cone (Sonic Concepts) filled with degassed water and sealed with an elastic membrane was inflated to achieve the correct axial distance from the target. NgFUS targeting was guided by the neuronavigation system (Brainsight System, Rogue Research Inc., Canada) (table S3).

The patients were positioned in a phlebotomy chair leaning forward with their head supported by an ophthalmology chinrest or a cushioned headrest depending on patient comfort. The patient's head was cleanly shaved in a circular area of ~10-cm radius at the sonication site, and water-based degassed ultrasound gel was applied directly onto the scalp to improve the transducer's coupling. The FUS transducer, supported by a mounted positioning arm, was manually guided to the preplanned sonication site using Brainsight's site targeting functionality. Once the transducer trajectory was within 2 mm and less than 20° of the planned target trajectory, the water-based ultrasound gel was applied to the elastic membrane. The transducer was then realigned to minimize error. Before initiation of sonication, a baseline cavitation signal was collected. The DEFINITY (Lantheus Medical Imaging, North Billerica, MA) microbubble vial was activated, as per the manufacturer's recommendation, and drawn up in a syringe shortly before sonication. DEFINITY microbubbles were administered at a dose of 10 μl/kg. The patient's port was cleared with a saline flush, and the syringe with microbubbles was attached. At the start of treatment, the microbubbles were injected ~3 s after the initiation of the sonication into the Port-a-Cath, which was immediately flushed with saline. Each sonication lasted for 2 min during which the cavitation signal was monitored in real time by the attending pediatric neuro-oncologist or radiation oncologist (*42*). For 2 NOTS sonications, the transducer was retargeted to the second preplanned trajectory using the neuronavigation system, with the second site sonication being initiated within 5 min of the conclusion of the first site sonication to minimize the loss of circulating microbubbles.

### Treatment planning and targeting

Patient-specific skull insertion loss coefficient of the FUS pressure for the planned beam trajectory was estimated before treatment to adjust the output power of FUS for each target (*42*). The patient's skull density and speed of sound maps were acquired through head computed tomography (CT) scans. The treatment planning MRI was anatomically registered with the prior CT scan. The tumor targets were identified on the MRI, and the simulation was performed on the CT scan. 3D numerical simulations were performed in MATLAB (The MathWorks, Natick, MA, USA) using the k-Wave acoustics toolbox (*43*–*45*) (data file S3). At least 10 simulations were performed per tumor site with variations of 2-mm Euclidean error and 20° angular error (*46*). Using the insertion loss coefficient, the transmit pressure of the transducer was adjusted so that the treatment would deliver an estimated peak-negative pressure of 200 kPa at the targeted site. The insertion loss coefficient used on the day of treatment was selected from the simulated values.

### Magnetic resonance imaging

The MRI protocol followed the Children's Hospital of New York (CHONY) Radiology Department's brain tumor imaging protocol for MRI with and without gadolinium contrast (Gadavist). MRI images were acquired within 1 to 4 hours after FUS treatment. Postcontrast fast spine echo T1-weighted and volume 3D MRI sequences were acquired ~10 to 15 min after injection of contrast. Identification of linear enhancement between pre-FUS and post-FUS volumetric postcontrast T1-weighted images was used to evaluate changes in BBB permeability. The BBBO volume was quantified by first registering the pre-FUS and post-FUS postcontrast MRI volumes. The pre-FUS volume was then subtracted from the post-FUS volume to isolate the difference in contrast enhancement resulting from the FUS procedure. The region of enhancement in the subtraction volume was manually contoured, and the volume of opening was computed automatically by thresholding the intensity values of the BBBO voxels until the mean value of the BBBO voxels was greater than the non-BBBO voxels within the selected region. The confidence interval was obtained from the *z*-scores assuming a Gaussian distribution of voxel intensities in the selected region. For example, a confidence interval of 95% corresponds to a factor of 1.96 and the threshold was found to separate the mean of BBBO voxels from the mean of the surrounding non-BBBO voxels by a difference of the SD of the surrounding non-BBBO voxels multiplied by 1.96 (*42*, *47*). The percent contrast enhancement was calculated by anatomically registering the pre-FUS MRI with the post-FUS MRI and comparing the mean intensity of the BBBO volume in post-FUS MRI with the mean intensity of the same volume in pre-FUS MRI. All MRIs were reviewed by a dedicated neuroradiologist and by a multidisciplinary team of neuro-oncologists and neuroradiologists at the weekly CUIMC Pediatric Neuro-Oncology Tumor Board.

### Cavitation dose

Real-time cavitation monitoring provides the monitoring physician with information on the microbubble cavitation magnitude, duration, and mode within the focal volume, as previously described (*41*, *47*). The doses for three modes of cavitation were calculated for the response of each pulse of the 120-pulse sonication. The three modes of SCDh, SCDu, and the ICD occupy unique regions of the frequency spectrum, and their magnitude indicates the strength of

certain microbubble oscillation patterns. Cavitation signals were detected using a concentrically aligned 1.5-MHz PCD (diameter: 32 mm, focal depth: 114 mm, sampling frequency: 50 MHz, capture length: 10 ms, ndtXducer, Northborough, MA, USA) and processed in MATLAB or a P4-2 array transducer (64 elements, center frequency: 2.5 MHz, bandwidth: 2 to 4 MHz, sampling frequency: 10 MHz, capture length: 10 ms by ATL Phillips, WA, USA) and processed in Verasonics Vantage 256 (Verasonics Inc., Kirkland, WA) (*47*). The SCDh and SCDu were determined by the averaged peak magnitudes of the third to sixth harmonic/ultraharmonic frequencies, whereas the ICD was calculated on the basis of the average magnitude within the 85-kHz bandwidth between the harmonic and ultraharmonic frequencies.

### Targeting precision assessment

The patient's movement relative to the transducer was tracked and recorded during sonication using the Brainsight neuronavigation system. For each sonication session, the maximum distance and MAD of the tracked FUS focal positions from the target centroid were obtained. The mean and SD of the maximum distance and MAD across all sessions were calculated to evaluate targeting precision.

### Statistical analysis

For the preclinical work, Student's *t* test and two-way analysis of variance (ANOVA) with post hoc tests were performed. For survival experiments, Kaplan-Meier survival analysis was used. All individual-level data are available in data file S4. For the clinical trial, individual patient-level results were presented along with descriptive statistics.

## Supplementary Materials

**The PDF file includes:**
Figs. S1 to S4
Tables S1 to S3

**Other Supplementary Material for this manuscript includes the following:**
Data files S1 to S4
MDAR Reproducibility Checklist

## REFERENCES AND NOTES


1. C. S. Grasso, Y. Tang, N. Truffaux, N. E. Berlow, L. Liu, M. A. Debily, M. J. Quist, L. E. Davis, E. C. Huang, P. J. Woo, A. Ponnuswami, S. Chen, T. B. Johung, W. Sun, M. Kogiso, Y. Du, L. Qi, Y. Huang, M. Hutt-Cabezas, K. E. Warren, L. Le Dret, P. S. Meltzer, H. Mao, M. Quezado, D. G. van Vuurden, J. Abraham, M. Fouladi, M. N. Svalina, N. Wang, C. Hawkins, J. Nazarian, M. M. Alonso, E. H. Raabe, E. Hulleman, P. T. Spellman, X. N. Li, C. Keller, R. Pal, J. Grill, M. Monje, Functionally defined therapeutic targets in diffuse intrinsic pontine glioma. *Nat. Med.* **21**, 827 (2015).
2. B. T. Himes, L. Zhang, D. J. Daniels, Treatment strategies in diffuse midline gliomas with the H3K27M mutation: The role of convection-enhanced delivery in overcoming anatomic challenges. *Front. Oncol.* **9**, 31 (2019).
3. M. Gallitto, S. Lazarev, I. Wasserman, J. M. Stafford, S. L. Wolden, S. A. Terezakis, R. S. Bindra, R. L. Bakst, Role of radiation therapy in the management of diffuse intrinsic pontine glioma: A systematic review. *Adv. Radiat. Oncol.* **4**, 520–531 (2019).
4. E. Subashi, F. J. Cordero, K. G. Halvorson, Y. Qi, J. C. Nouls, O. J. Becher, G. A. Johnson, Tumor location, but not H3.3K27M, significantly influences the blood-brain-barrier permeability in a genetic mouse model of pediatric high-grade glioma. *J. Neurooncol.* **126**, 243–251 (2016).
5. R. Zhao, G. M. Pollack, Regional differences in capillary density, perfusion rate, and P-glycoprotein activity: A quantitative analysis of regional drug exposure in the brain. *Biochem. Pharmacol.* **78**, 1052–1059 (2009).
6. D. Gomez-Zepeda, M. Taghi, J. M. Scherrmann, X. Decleves, M. C. Menet, ABC transporters at the blood-brain interfaces, their study models, and drug delivery implications in gliomas. *Pharmaceutics* **12**, 20 (2019).
7. W. M. Pardridge, The blood-brain barrier: Bottleneck in brain drug development. *NeuroRx* **2**, 3–14 (2005).
8. C. Chaves, X. Decleves, M. Taghi, M. C. Menet, J. Lacombe, P. Varlet, N. G. Olaciregui, A. M. Carcaboso, S. Cisternino, Characterization of the blood-brain barrier integrity and the brain transport of SN-38 in an orthotopic xenograft rat model of diffuse intrinsic pontine glioma. *Pharmaceutics* **12**, 399 (2020).
9. L. M. Arms, R. J. Duchatel, E. R. Jackson, P. G. Sobrinho, M. D. Dun, S. Hua, Current status and advances to improving drug delivery in diffuse intrinsic pontine glioma. *J. Control. Release* **370**, 835–865 (2024).
10. Y. Meng, K. Hynynen, N. Lipsman, Applications of focused ultrasound in the brain: From thermoablation to drug delivery. *Nat. Rev. Neurol.* **17**, 7–22 (2021).
11. E. E. Konofagou, Y.-S. Tung, J. Choi, T. Deffieux, B. Baseri, F. Vlachos, Ultrasound-induced blood-brain barrier opening. *Curr. Pharm. Biotechnol.* **13**, 1332–1345 (2012).
12. K. Parekh, S. LeBlang, J. Nazarian, S. Mueller, S. Zacharoulis, K. Hynynen, L. Powlovich, Past, present and future of focused ultrasound as an adjunct or complement to DIPG/DMG therapy: A consensus of the 2021 FUSF DIPG meeting. *Neoplasia* **37**, 100876 (2023).
13. Z. K. Englander, H. J. Wei, A. N. Pouliopoulos, E. Bendau, P. Upadhyayula, C. I. Jan, E. F. Spinazzi, N. Yoh, M. Tazhibi, N. M. McQuillan, T. J. C. Wang, J. N. Bruce, P. Canoll, N. A. Feldstein, S. Zacharoulis, E. E. Konofagou, C. C. Wu, Focused ultrasound mediated blood-brain barrier opening is safe and feasible in a murine pontine glioma model. *Sci. Rep.* **11**, 6521 (2021).
14. N. Yoh, M. Tazhibi, Z. Englander, C.-C. Wu, G. Baltuch, Focused ultrasound for ablation in neurosurgery—Present use and future directions. *Appl. Radiat. Oncol.* **11**, 14–22 (2022).
15. T. Hennika, G. Hu, N. G. Olaciregui, K. L. Barton, A. Ehteda, A. Chitranjan, C. Chang, A. J. Gifford, M. Tsoli, D. S. Ziegler, A. M. Carcaboso, O. J. Becher, Pre-clinical study of panobinostat in xenograft and genetically engineered murine diffuse intrinsic pontine glioma models. *PLOS ONE* **12**, e0169485 (2017).
16. M. Monje, T. Cooney, J. Glod, J. Huang, C. J. Peer, D. Faury, P. Baxter, K. Kramer, A. Lenzen, N. J. Robison, L. Kilburn, A. Vinitsky, W. D. Figg, N. Jabado, M. Fouladi, J. Fangusaro, A. Onar-Thomas, I. J. Dunkel, K. E. Warren, Phase I trial of panobinostat in children with diffuse intrinsic pontine glioma: A report from the Pediatric Brain Tumor Consortium (PBTC-047). *Neuro Oncol.* **25**, 2262–2272 (2023).
17. K. Lehrfeld, "The Food and Drug Administration (FDA or Agency) is withdrawing approval of the new drug application (NDA) for FARYDAK (panobinostat) capsules, 10 milligrams (mg), 15 mg, and 20 mg, held by Secura Bio, Inc." (Federal Register, 2022).
18. A. M. Sonabend, A. Gould, C. Amidei, R. Ward, K. A. Schmidt, D. Y. Zhang, C. Gomez, J. F. Bebawy, B. P. Liu, G. Bouchoux, C. Desseaux, I. B. Helenowski, R. V. Lukas, K. Dixit, P. Kumthekar, V. A. Arrieta, M. S. Lesniak, A. Carpentier, H. Zhang, M. Muzzio, M. Canney, R. Stupp, Repeated blood-brain barrier opening with an implantable ultrasound device for delivery of albumin-bound paclitaxel in patients with recurrent glioblastoma: A phase 1 trial. *Lancet Oncol.* **24**, 509–522 (2023).
19. A. R. Rezai, P. F. D'Haese, V. Finomore, J. Carpenter, M. Ranjan, K. Wilhelmsen, R. I. Mehta, P. Wang, U. Najib, C. Vieira Ligo Teixeira, T. Arsiwala, A. Tarabishy, P. Tirumalai, D. O. Claassen, S. Hodder, M. W. Haut, Ultrasound blood-brain barrier opening and aducanumab in Alzheimer's disease. *N. Engl. J. Med.* **390**, 55–62 (2024).
20. S. Alli, C. A. Figueiredo, B. Golbourn, N. Sabha, M. Y. Wu, A. Bondoc, A. Luck, D. Coluccia, C. Maslink, C. Smith, H. Wurdak, K. Hynynen, M. O'Reilly, J. T. Rutka, Brainstem blood brain barrier disruption using focused ultrasound: A demonstration of feasibility and enhanced doxorubicin delivery. *J. Control. Release* **281**, 29–41 (2018).
21. J. Ishida, S. Alli, A. Bondoc, B. Golbourn, N. Sabha, K. Mikloska, S. Krumholtz, D. Srikanthan, N. Fujita, A. Luck, C. Maslink, C. Smith, K. Hynynen, J. Rutka, MRI-guided focused ultrasound enhances drug delivery in experimental diffuse intrinsic pontine glioma. *J. Control. Release* **330**, 1034–1045 (2021).
22. P. Martinez, G. Nault, J. Steiner, M. F. Wempe, A. Pierce, B. Brunt, M. Slade, J. J. Song, A. Mongin, K. H. Song, N. Ellens, N. Serkova, A. L. Green, M. Borden, MRI-guided focused ultrasound blood-brain barrier opening increases drug delivery and efficacy in a diffuse midline glioma mouse model. *Neurooncol. Adv.* **5**, vdad111 (2023).
23. H. J. Wei, A. Pouliopoulos, N. Yoh, M. Tazhibi, N. McQuillan, X. Zhang, L. Szalontay, R. Gartrell, P. Jovana, Z. Zhang, N. Feldstein, S. Zacharoulis, E. E. Konofagou, C. C. Wu, Focused ultrasound-mediated blood-brain barrier opening enhances panobinostat efficacy in a murine diffuse intrinsic pontine glioma model. *Int. J. Radiat. Oncol. Biol. Phys.* **111**, e177 (2021).
24. K. B. Leszczynska, C. Jayaprakash, B. Kaminska, J. Mieczkowski, Emerging advances in combinatorial treatments of epigenetically altered pediatric high-grade H3K27M gliomas. *Front. Genet.* **12**, 742561 (2021).
25. L. T. Rodgers, C. M. Lester McCully, A. Odabas, R. Cruz, C. J. Peer, W. D. Figg, K. E. Warren, Characterizing the pharmacokinetics of panobinostat in a non-human primate model for the treatment of diffuse intrinsic pontine glioma. *Cancer Chemother. Pharmacol.* **85**, 827–830 (2020).
26. A. Carpentier, R. Stupp, A. M. Sonabend, H. Dufour, O. Chinot, B. Mathon, F. Ducray, J. Guyotat, N. Baize, P. Menei, J. de Groot, J. S. Weinberg, B. P. Liu, E. Guemas, C. Desseaux, C. Schmitt, G. Bouchoux, M. Canney, A. Idbaih, Repeated blood-brain barrier opening

with a nine-emitter implantable ultrasound device in combination with carboplatin in recurrent glioblastoma: A phase I/II clinical trial. *Nat. Commun.* **15**, 1650 (2024).
27. A. Burgess, K. Shah, O. Hough, K. Hynynen, Focused ultrasound-mediated drug delivery through the blood-brain barrier. *Expert Rev. Neurother.* **15**, 477–491 (2015).
28. S. Schoen Jr., M. S. Kilinc, H. Lee, Y. Guo, F. L. Degertekin, G. F. Woodworth, C. Arvanitis, Towards controlled drug delivery in brain tumors with microbubble-enhanced focused ultrasound. *Adv. Drug Deliv. Rev.* **180**, 114043 (2022).
29. P. Y. Lee, H. J. Wei, A. N. Pouliopoulos, B. T. Forsyth, Y. Yang, C. Zhang, A. F. Laine, E. E. Konofagou, C. C. Wu, J. Guo, Deep learning enables reduced gadolinium dose for contrast-enhanced blood-brain barrier opening. arXiv:2301.07248 [q-bio.QM] (2023).
30. M. E. M. Stamp, M. Halwes, D. Nisbet, D. J. Collins, Breaking barriers: Exploring mechanisms behind opening the blood-brain barrier. *Fluids Barriers CNS* **20**, 87 (2023).
31. A. R. Kline-Schoder, S. Chintamen, M. J. Willner, M. R. DiBenedetto, R. L. Noel, A. J. Batts, N. Kwon, S. Zacharoulis, C. C. Wu, V. Menon, S. G. Kernie, E. E. Konofagou, Characterization of the responses of brain macrophages to focused ultrasound-mediated blood-brain barrier opening. *Nat. Biomed. Eng.* **8**, 650–663 (2024).
32. ClinicalTrials.gov, FUS Etoposide for DMG; https://clinicaltrials.gov/study/NCT05762419.
33. K. Melde, A. G. Mark, T. Qiu, P. Fischer, Holograms for acoustics. *Nature* **537**, 518–522 (2016).
34. S. Jiménez-Gambin, N. Jimenez, J. M. Benlloch, F. Camarena, in *International Congress on Ultrasonics* (European Acoustics Association, 2019), vol. 38, pp. 020013.
35. S. Jiménez-Gambín, A. N. Pouliopoulos, Z. K. Englander, N. Jiménez, F. Camarena, E. E. Konofagou, S. Zacharoulis, C. C. Wu, in *2021 IEEE International Ultrasonics Symposium (IUS)* (IEEE, 2021), pp. 1–4.
36. S. Jimenez-Gambin, N. Jimenez, A. Pouliopoulos, J. M. Benlloch, E. Konofagou, F. Camarena, Acoustic holograms for bilateral blood-brain barrier opening in a mouse model. *IEEE Trans. Biomed. Eng.* **69**, 1359–1368 (2022).
37. M. Johnson, "This 6-year-old is a pioneer in the quest to treat a deadly brain tumor," *The Washington Post*, 25 September 2023.
38. E. C. Fernandez, L. Tomassoni, X. Zhang, J. Wang, A. Obradovic, P. Laise, A. T. Griffin, L. Vlahos, H. E. Minns, D. V. Morales, C. Simmons, M. Gallitto, H. J. Wei, T. J. Martins, P. S. Becker, J. R. Crawford, T. Tzaridis, R. J. Wechsler-Reya, J. Garvin, R. D. Gartrell, L. Szalontay, S. Zacharoulis, C. C. Wu, Z. Zhang, A. Califano, J. Pavisic, Elucidation and pharmacologic targeting of master regulator dependencies in coexisting diffuse midline glioma subpopulations. bioRxiv 2024.03.17.585370 [Preprint] (2024). https://doi.org/10.1101/2024.03.17.585370.
39. M. Tazhibi, N. McQuillan, H. J. Wei, M. Gallitto, E. Bendau, A. Webster Carrion, X. Berg, D. Kokossis, X. Zhang, Z. Zhang, C. I. Jan, A. Mintz, R. D. Gartrell, H. R. Syed, A. Fonseca, J. Pavisic, L. Szalontay, E. E. Konofagou, S. Zacharoulis, C. C. Wu, Focused ultrasound-mediated blood-brain barrier opening is safe and feasible with moderately hypofractionated radiotherapy for brainstem diffuse midline glioma. *J. Transl. Med.* **22**, 320 (2024).
40. A. N. Pouliopoulos, S. Y. Wu, M. T. Burgess, M. E. Karakatsani, H. A. S. Kamimura, E. E. Konofagou, A clinical system for non-invasive blood-brain barrier opening using a neuronavigation-guided single-element focused ultrasound transducer. *Ultrasound Med. Biol.* **46**, 73–89 (2020).
41. A. N. Pouliopoulos, N. Kwon, G. Jensen, A. Meaney, Y. Niimi, M. T. Burgess, R. Ji, A. J. McLuckie, F. A. Munoz, H. A. S. Kamimura, A. F. Teich, V. P. Ferrera, E. E. Konofagou, Safety evaluation of a clinical focused ultrasound system for neuronavigation guided blood-brain barrier opening in non-human primates. *Sci. Rep.* **11**, 15043 (2021).
42. S. Bae, K. Liu, A. N. Pouliopoulos, R. Ji, S. Jimenez-Gambin, O. Yousefian, A. R. Kline-Schoder, A. J. Batts, F. N. Tsitsos, D. Kokossis, A. Mintz, L. S. Honig, E. E. Konofagou, Transcranial blood-brain barrier opening in Alzheimer's disease patients using a portable focused ultrasound system with real-time 2-D cavitation mapping. medRxiv 2023.12.21.23300222 [Preprint] (2024). https://doi.org/10.1101/2023.12.21.23300222.
43. B. E. Treeby, B. T. Cox, Modeling power law absorption and dispersion for acoustic propagation using the fractional Laplacian. *J. Acoust. Soc. Am.* **127**, 2741–2748 (2010).
44. B. E. Treeby, J. Jaros, A. P. Rendell, B. T. Cox, Modeling nonlinear ultrasound propagation in heterogeneous media with power law absorption using a k-space pseudospectral method. *J. Acoust. Soc. Am.* **131**, 4324–4336 (2012).
45. B. E. Treeby, B. T. Cox, k-Wave: MATLAB toolbox for the simulation and reconstruction of photoacoustic wave fields. *J. Biomed. Opt.* **15**, 021314 (2010).
46. S. Jimenez-Gambin, S. Bae, R. Ji, F. Tsitsos, E. E. Konofagou, Feasibility of hologram-assisted bilateral blood-brain barrier opening in non-human primates. *IEEE Trans. Ultrason. Ferroelectr. Freq. Control* **71**, 1172–1185 (2024).
47. S. Bae, K. Liu, A. N. Pouliopoulos, R. Ji, E. E. Konofagou, Real-time passive acoustic mapping with enhanced spatial resolution in neuronavigation-guided focused ultrasound for blood-brain barrier opening. *IEEE Trans. Biomed. Eng.* **70**, 2874–2885 (2023).

**Acknowledgments**
**Funding:** This study was supported by the Gary Yael Fegel Foundation (C.-C.W., L.S., J.P., and S.Z.); Focused Ultrasound Foundation (C.-C.W., K.S., S.Z., and E.E.K.); St. Baldrick's Foundation (C.-C.W. and L.S.); Hannah's Heroes (C.-C.W.), Sebastian Strong Foundation (C.-C.W.); Swim Across America (C.-C.W., J.P., and R.D.G.); Matheson Foundation (C.-C.W.); Pediatric Cancer Foundation (C.-C.W., J.P., R.D.G., and S.Z.); Hope and Heroes (C.-C.W., L.S., and S.Z.); Team Jack Foundation (C.-C.W., L.S., and J.P.); Hyundai Hope on Wheels Hope Scholar Award (R.D.G.); Rally Foundation (R.D.G.); Stache Strong Foundation (R.D.G.); Musella Foundation (R.D.G.); VP&S Interdisciplinary Research Initiative Seed Grant (C.-C.W. and J.P.); National Institutes of Health grants R01AG03861 (E.E.K.), R01EB029338 (E.E.K.), and R56AG038961 (E.E.K.); Red Gate Foundation (C.-C.W.); and Alzheimer's Disease Research Center (ADRC) Research Education (REC) Program (S.B.). **Author contributions:** C.-C.W., E.E.K., S.Z., H.-J.W., and A.N.P. participated in the conceptualization of the study. C.-C.W., E.E.K., S.Z., H.-J.W., L.S., and A.N.P. developed the methodology. C.-C.W., S.Z., L.S., X.B., C.S., J.F., H.S., R.J., S.B., G.D.L.S., M.T., N.M., A.W.C., O.Y., D.K., M.G., N.Y., Z.E., P.C., A.M., A.L., and N.F. participated in the investigation of the preclinical and clinical trial. C.-C.W., S.Z., L.S., S.B., X.B., and D.K. participated in the visualization. Funding support for this study was obtained by C.-C.W., S.Z., E.E.K., L.S., R.G., and J.P. The administration of the project was performed by C.-C.W., S.Z., L.S., C.S., H.S., and R.D.G. The trial was supervised by C.-C.W., S.Z., L.S., and J.G. C.-C.W., E.E.K., A.N.P., S.B., X.B., R.J., Z.J., H.-J.W., J.F., and A.W.C. participated in the writing of the original draft. C.-C.W., J.L., J.G., H.W., S.Z., S.B., R.J., R.G., L.S., and E.E.K. participated in the writing for the review and editing. **Competing interests:** E.E.K. is a cofounder of Delsona Therapeutics Inc. (Wilmington, DE) and serves as a coinventor on patents that may be related to the technologies presented herein. List of patents below. E.E.K. has filed patents related to this work ("Systems and methods for opening tissues," US-20220273929-A1; "Systems and methods for opening of a tissue barrier in primates," US-20220193457-A1; "Systems and methods for opening of a tissue barrier in primates," US-11273329-B2; "Systems and methods for opening of a tissue barrier in primates," US-20200086146-A1; "Systems and methods for opening of a tissue barrier in primates," US-10441820-B2; "Systems and methods for real-time, transcranial monitoring of blood-brain barrier opening," US-20190192112-A1; "Systems and methods for targeted drug delivery," US-10322178-B2; "Systems and methods for non-invasive brain stimulation with ultrasound," US-20190090738-A1; "Systems and methods for opening of a tissue barrier," US-10166379-B2; "Systems and methods for opening of a tissue barrier," US-10166379-B2; "Systems and methods for real-time, transcranial monitoring of blood-brain barrier opening," US-10166379-B2; "Systems and methods for opening of a tissue barrier," US-10166379-B2; "Systems and methods for real-time, transcranial monitoring of blood-brain barrier opening," US-10028723-B2; "Systems and methods for opening of a tissue barrier," US-20160346526-A1; "Ultrasound devices methods and systems," US-20160296203-A1; "Systems and methods for opening a tissue," US-20160287856-A1; "System and method for electromechanical activation of arrhythmias," US-20160249880-A1; "Systems and methods for non-invasive brain stimulation with ultrasound," US-20160242648-A1; "Systems and methods for opening of a tissue barrier," US-9358023-B2; "Systems and methods for opening a tissue," US-9302124-B2; "Systems and methods for real-time, transcranial monitoring of blood-brain barrier opening," US-20150065871-A1; "Systems and methods for targeted drug delivery," US-20150045724-A1; "Systems and methods of high frame rate streaming for treatment monitoring," US-20150010222-A1; "Systems and methods for opening of a tissue barrier in primates," US-20140114216-A1; "Medical imaging contrast devices, methods, and systems," US-20130289398-A1; "Systems and methods for opening of a tissue barrier," US-20130046229-A1; "Systems and methods for opening a tissue," US-20110295105-A1; "Systems and methods for opening of the blood-brain barrier of a patient using ultrasound," US-20090005711-A1). Information regarding technology under patent can be obtained by contacting E.E.K. C.-C.W. is an adviser for the DIGP/DMG National Tumor Board. All other authors declare that they have no competing interests. **Data and materials availability:** All data and materials associated with this study are present in the paper or the Supplementary Materials. The focused ultrasound device IP is owned by Delsona. The device is not commercially available but is available for clinical trials. E.E.K. can be contacted for material/device transfer agreement. For material transfer agreement requests, please contact technventures@columbia.edu.

Submitted 28 May 2024
Resubmitted 5 November 2024
Accepted 1 October 2025
Published 12 November 2025
10.1126/scitranslmed.adq6645